J|A|C|S
ARTICLES
Published on Web 05/06/2005

Surface Layering in Ionic Liquids: An X-ray Reflectivity Study

Eli Solutskin,[†] Benjamin M. Ocko,[‡] Lilach Taman,[†] Ivan Kuzmenko,[§] Thomas Gog,[§] and Moshe Deutsch*,[†]

Contribution from the Department of Physics, Bar-Ilan University, Ramat-Gan 52900, Israel, Department of Physics, Brookhaven National Laboratory, Upton, New York 11973, CMC-CAT, Advanced Photon Source, Argonne National Lab, Illinois 60439

Received February 15, 2005; E-mail: deutsch@mail.biu.ac.il

Abstract: The surface structure and thermodynamics of two ionic liquids, based on the 1-alkyl-3-methylimidazolium cations, were studied by X-ray reflectivity and surface tensiometry. A molecular layer of a density ~18% higher than that of the bulk is found to form at the free surface of these liquids. In common with surface layering in liquid metals and surface freezing in melts of organic chain molecules, this effect is induced by the lower dimensionality of the surface. The concentrations of the oppositely charged ions within the surface layer are determined by chemical substitution of the anion. The temperature-dependent surface tension measurements reveal a normal, negative-slope temperature dependence. The different possible molecular arrangements within the enhanced-density surface layer are discussed.

I. Introduction

Ionic liquids[1] (ILs) are melts of salts which have much lower melting points than normal salts, usually $\lesssim$100 °C. In contrast with salt *solutions*, the ILs consist solely of ions, without the presence of any solvent. In several classes of ILs, the bulky and asymmetric shape of the cation destabilizes the crystalline lattice, reducing the melting temperature (and increasing the liquidus range) of the ILs by hundreds of degrees, as compared to classical salts having single or few-atom cations and anions, such as NaCl, $ZnBr_2$, or $NaNO_3$. ILs are nonvolatile, nonflammable, and thermally stable solvents and as such are promising "green" replacements for traditional volatile organic solvents. At present the number of ILs synthesized[2] exceeds 500. Due to the ILs' great industrial potential,[1,3] this number is growing at an exceedingly fast rate.

In a macroscopic sample, the number of molecules composing the surface phase is smaller by tens of orders of magnitude than the number of bulk molecules. Despite this great disparity, surfaces and interfaces determine many important properties of macroscopic matter, such as the solubility,[4] the extent of liquid supercooling,[5−7] the vapor pressure,[8] and many more. All chemical reactions are set off and catalyzed at interfaces between the participating species. The physical properties of the surface phase, e.g. the free energy,[9] the concentrations in mixtures and solutions,[4,10,11] are different in the general case from those of the bulk phase. A good example for that is the surface freezing (SF) effect of single-component melts of linear-chain alkanes[12] ($CH_3(CH_2)_{n-2}CH_3$, $16 \le n \le 50$) and some of their derivatives.[13,14] This effect consists of the formation of a crystalline monolayer (in alkanes) or bilayer (in alcohols) at the free surface of the melt, several degrees above the bulk melting temperature. Some of the theories put forth to account for the SF effect indicate that the anisotropic, rodlike structure of the alkane molecules is an essential ingredient for the occurrence of SF.[15]

[†] Bar-Ilan University.
[‡] Brookhaven National Laboratory.
[§] Argonne National Lab.

(1) Rogers, R. D.; Seddon, K. R. *Science* **2003**, *302*, 792−793. Xu, W.; Angell, C. A. *Science* **2003**, *302*, 422−425. Seddon, K. R. *Nat. Mater.* **2003**, *2*, 363−365.
(2) Marsh, K. N.; Boxall, J. A.; Lichtenthaler, R. *Fluid Phase Equilib.* **2004**, *219*, 93−98.
(3) Cooper, E. R.; Andrews, C. D.; Wheatley, P. S.; Webb, P. B.; Wormald, P.; Morris, R. E. *Nature* **2004**, *430*, 1012−1016. Senadeera, G. K. R.; Pathirathne, W. M. T. C. *Curr. Sci.* **2004**, *87*, 339−342. *Chem. Eng. News* **2003**, *81*(13), 9.
(4) Guggenheim, E. A. *Mixtures*; Oxford University Press: Oxford, 1952.
(5) Sloutskin, E.; Sirota, E. B.; Kraack, H.; Ocko, B. M.; Deutsch, M. *Phys. Rev. E* **2001**, *64*, 031708
(6) Kraack, H.; Sirota, E. B.; Deutsch, M. *Polymer* **2001**, *42*, 8225−8233. Zhong, J.; Jin, Z. H.; Lu, K. *J. Phys.: Condens. Matter* **2001**, *13*, 11443−11452.
(7) Sloutskin, E.; Bain, C. D.; Ocko, B. M.; Deutsch, M. *Faraday Discuss.* **2005**, *129*, 339−352.
(8) Bunyakan, C.; Malakarn, S.; Tongurai, C. *Songklanakarin J. Sci. Technol.* **2002**, *24*, 255−271. O'Brien, R. N.; Feher, A. I.; Li, K. L.; Tan, W. C. *Can. J. Chem.* **1976**, *54*, 2739−2744.
(9) Hildebrand, J. H.; Scott, R. L. *The Solubility of Nonelectrolytes*; Reinhold: New York, 1950.
(10) Sloutskin, E.; Gang, O.; Kraack, H.; Ocko, B. M.; Sirota, E. B.; Deutsch, M. *Phys. Rev. Lett.* **2002**, *89*, 065501. Sloutskin, E.; Sirota, E. B.; Gang, O.; Wu, X. Z.; Ocko, B. M.; Deutsch, M. *Eur. Phys. J. E (Rapid)* **2004**, *13*, 109−112.
(11) Sloutskin, E.; Wu, X. Z.; Peterson, T. B.; Gang, O.; Ocko, B. M.; Sirota, E. B.; Deutsch, M. *Phys. Rev. E* **2003**, *68*, 031605. Sloutskin, E.; Gang, O.; Kraack, H.; Sirota, E. B.; Ocko, B. M.; Deutsch, M. *Phys. Rev. E* **2003**, *68*, 031606. Sloutskin, E.; Sirota, E. B.; Kraack, H.; Gang, O.; Doerr, A.; Ocko, B. M.; Deutsch, M. *J. Chem. Phys.* **2002**, *116*, 8056−8066.
(12) Ocko, B. M.; Wu, X. Z.; Sirota, E. B.; Sinha, S. K.; Gang, O.; Deutsch, M. *Phys. Rev. E* **1997**, *55*, 3164−3182.
(13) Gang, O.; Wu, X. Z.; Ocko, B. M.; Sirota, E. B.; Deutsch, M. *Phys. Rev. E* **1998**, *58*, 6086−6100. Gang, O.; Ocko, B. M.; Wu, X. Z.; Sirota, E. B.; Deutsch, M. *Phys. Rev. Lett.* **1998**, *80*, 1264−1267.
(14) Sloutskin, E.; Kraack, H.; Ocko, B. M.; Ellmann, J.; Möller, M.; Lo Nostro, P.; Deutsch, M. *Langmuir* **2002**, *18*, 1963−1967. Gang, O.; Ellmann, J.; Möller, M.; Kraack, H.; Sirota, E. B.; Ocko, B. M.; Deutsch, M.; *Europhys. Lett.* **2000**, *49*, 761−767. Gang, O.; Ocko, B. M.; Wu, X. Z.; Sirota, E. B.; Deutsch, M. *Phys. Rev. Lett.* **1999**, *82*, 588−591.
(15) Tkachenko, A. V.; Rabin, Y. *Phys. Rev. Lett.* **1996**, *76*, 2527−2530. Tkachenko, A. V.; Rabin, Y. *Phys. Rev. E* **1997**, *55*, 778−784. Sirota, E. B.; Wu, X. Z.; Ocko, B. M.; Deutsch, M. *Phys. Rev. Lett.* **1997**, *79*, 531. Tkachenko, A. V.; Rabin, Y. *Phys. Rev. Lett.* **1997**, *79*, 532. Mukherjee, P. K.; Deutsch, M. *Phys. Rev. E* **2000**, *61*, 637−641.

10.1021/ja0509679 CCC: $30.25

Recent studies reveal effects similar to SF at liquid−liquid[7,16] and solid−air[17] interfaces involving alkanes. Surface-induced ordering was also detected in liquid crystals (LC), where smectic surface layers, often extending hundreds of angstroms into the bulk, coexist with either a nematic or an isotropic bulk.[18]

The surfaces of liquid metals (Hg, K, In, Ga, etc.), consisting of classical Coulombic interacting ions, screened by a Fermi quantum liquid of free electrons, also exhibit a characteristic surface layering (SL) effect, yielding an oscillatory surface-normal density profile.[19,20] The layering is not confined to high surface tension (ST) liquid metals such as mercury (∼500 mN/m) or gallium (∼750 mN/m). It has also been detected in low ST liquid metals, such as potassium,[21] the ST of which (110 mN/m) is close to that of water (72 mN/m), which does not exhibit SL.[22] The most likely reason for the SL effect is the interplay between the classical ion liquid and the quantum fluid of free electrons.[23] The possibility of surface layering in nonmetallic liquids is currently under a vigorous debate.[24,25]

A key question concerning the surface-ordering phenomena is whether a common denominator can be found for SL in liquid metals, surface freezing in the normal alkanes and surface ordering in LC. In ILs, the alkyl tails resemble the normal alkanes, the heterocyclic rings in the ILs resemble the polar LC headgroups, and the solvent-free oppositely charged two-ion structure of ILs resembles the negative electron−positive ion structure of liquid metals. Thus, the ILs seem to be a good choice to search for common physics underlying the various surface-ordering phenomena. Atomistic simulations of particular ILs[26] indicate that SL, akin to that of liquid metals, indeed occurs in those ILs. Note, however, that these simulations address dimethyl-imidazolium chloride, which does not have long alkyl tails. The ILs chosen for the present study are the 1-butyl-3-methylimidazolium hexafluorophosphate ([bmim][PF_6]) and 1-butyl-3-methylimidazolium tetrafluoroborate ([bmim][BF_4]), both having the same [bmim]$^+$ cation but different anion structures, as shown in Figure 1. Recent neutron reflectivity studies[27] indicate possible surface layering in [bmim][BF_4].

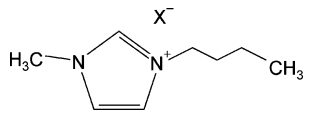

Figure 1. Molecular structure of [bmim][X], where X^- is the BF_4^- or the PF_6^- anion, respectively. The positional probability density of the anion in the liquid state is almost spherically symmetric with respect to the center of the imidazolium ring. The highest probability, however, is obtained over the C(2) carbon atom,[28] i.e., the carbon atom located between the two N atoms of the imidazolium ring.

However, the low neutron flux (orders of magnitude lower than that of X-rays at a synchrotron source) and consequently the limited measurement range did not allow an unambiguous proof for the existence of layering and for determining its various characteristics in that study.

The bulk behavior of [bmim][BF_4] and of [bmim][PF_6] has been widely studied,[28−30] and many novel applications[31] involving these two materials were suggested and patented. The ST of [bmim][BF_4] and [bmim][PF_6] were measured in two earlier works[29,32] yielding qualitatively similar, though quantitatively different, results. Direct recoil spectroscopy (DRS)[33−35] and sum frequency generation spectroscopy (SFG)[36] studies were also carried out and determined the orientation of the surface layer molecules in these two ILs. However, the conclusions of these two studies are contradictory. The SFG indicates that the imidazolium ring of the cation is almost surface-parallel and the butyl tails protrude out of the surface. In contrast, the DRS results indicate that the plane of the imidazolium ring is perpendicular to the surface and the butyl tails are surface-parallel for [bmim][PF_6] and pointing into the bulk phase for [bmim][BF_4].[33]

Despite the immense importance of the surface and interface properties of ILs for technological applications, they were only little studied to date.[2,27,29,32−39] The present study addresses such

(16) Lei, Q.; Bain, C. D. *Phys. Rev. Lett.* **2004**, *92*, 176103.
(17) Merkl, C.; Pfohl, T.; Riegler, H. *Phys. Rev. Lett.* **1997**, *79*, 4625−4628. Maeda, N.; Kohonen, N. M.; Christenson, H. K. *Phys. Rev. E* **2000**, *61*, 7239−7242. Schollmeyer, H.; Struth, B.; Riegler, H. *Langmuir* **2003**, *19*, 5042−5051. Holzwarth, A.; Leporatti, S.; Riegler, H. *Europhys. Lett.* **2000**, *52*, 653−659. Yamamoto, Y.; Ohara, H.; Kajikawa, K.; Ishii, H.; Ueno, N.; Seki, K.; Ouchi, Y. *Chem. Phys. Lett.* **1999**, *304*, 231−235.
(18) Als-Nielsen, J.; Christensen, F.; Pershan, P. S. *Phys. Rev. Lett.* **1982**, *48*, 1107−1110. Ocko, B. M.; Braslau, A.; Pershan, P. S.; Als-Nielsen, J.; Deutsch, M. *Phys. Rev. Lett.* **1986**, *57*, 94−97.
(19) Magnussen, O. M.; Ocko, B. M.; Regan, M. J.; Penanen, K.; Pershan, P. S.; Deutsch, M. *Phys. Rev. Lett.* **1995**, *74*, 4444−4447. Regan, M. J.; Kawamoto, E. H.; Lee, S.; Pershan, P. S.; Maskil, N.; Deutsch, M.; Magnussen, O. M.; Ocko, B. M.; Berman, L. E. *Phys. Rev. Lett* **1995**, *75*, 2498−2501. Tostmann, H.; DiMasi, E.; Pershan, P. S.; Ocko, B. M.; Shpyrko, O. G.; Deutsch, M. *Phys. Rev. B* **1999**, *59*, 783−791.
(20) Regan, M. J.; Pershan, P. S.; Magnussen, O. M.; Ocko, B. M.; Deutsch, M.; Berman, L. E. *Phys. Rev. B* **1996**, *54*, 9730−9733.
(21) Shpyrko, O.; Huber, P.; Grigoriev, A.; Pershan, P. S.; Ocko, B. M.; Tostmann, H.; Deutsch, M. *Phys. Rev. B* **2003**, *67*, 115405.
(22) Shpyrko, O.; Fukuto, M.; Pershan, P. S.; Ocko, B. M.; Kuzmenko, I.; Gog, T.; Deutsch, M. *Phys. Rev. B* **2004**, *69*, 245423. Schwartz D. K.; Schlossman, M. L.; Kawamoto, E. H.; Kellogg, G. J.; Pershan, P. S.; Ocko, B. M. *Phys. Rev. A* **1990**, *41*, 5687−5690.
(23) Gómez, M. A.; Chacón, E. *Phys. Rev. B* **1992**, *46*, 723−732. Iwamatsu, M.; Lai, S. K. *J. Phys.: Condens. Matter* **1992**, *4*, 6039−6046. Evans, R.; Henderson, J. R.; Hoyle, D. C.; Parry, A. O.; Sabeur, Z. A. *Mol. Phys.* **1993**, *80*, 755−775.
(24) Chacón, E.; Reinaldo-Falagan, M.; Velasco, E.; Tarazona, P. *Phys. Rev. Lett.* **2001**, *87*, 166101. Velasco, E.; Tarazona, P.; Reinaldo-Falagan, M.; Chacón, E. *J. Chem. Phys.* **2002**, *117*, 10777−10788. Garrett, B. C. *Science* **2003**, *303*, 1146−1147. Shultz, M. J.; Baldelli, S.; Schnitzer, C.; Simonelli, D. *J. Phys. Chem. B* **2002**, *106*, 5313−5324.
(25) Li, D. X.; Rice, S. A. *J. Phys. Chem. B* **2004**, *108*, 19640−19646.
(26) Lynden-Bell, R. M. *Mol. Phys.* **2003**, *101*, 2625−2633.
(27) Bowers, J.; Vergara-Gutierrez, M. C.; Webster, J. R. P. *Langmuir* **2004**, *20*, 309−312.
(28) Anthony, J. L.; Crosthwaite, J. M.; Hert, D. G.; Aki, S. N. V. K.; Maginn, E. J.; Brennecke, J. F. ACS Symposium Series 856; American Chemical Society: Washington, DC, 2003; pp 110−120. Shah, J. K.; Maginn, E. J. *Fluid Phase Equilib.* **2004**, *222*, 195−203. Morrow, T. I.; Maginn, E. J. *J. Phys. Chem. B* **2002**, *106*, 12807−12813. Anthony, J. L.; Maginn, E. J.; Brennecke, J. F. *J. Phys. Chem. B* **2002**, *106*, 7315−7320. Shah, J.; Brennecke, J. F.; Maginn, E. J. *Green Chem.* **2002**, *4*, 112−118. Shröder, U.; Wadhawan, J. D.; Compton, R. G.; Marken, F.; Suarez, P. A. Z.; Consorti, C. S.; de Souza, R. F.; Dupont, J. *New J. Chem.* **2000**, *24*, 1009−1015.
(29) Huddleston, J. G.; Visser, A. E.; Reichert, W. M.; Willauer, H. D.; Broker, G. A.; Rogers, R. D. *Green Chem.* **2001**, *3*, 156−164.
(30) Holbrey, J. D.; Seddon, K. R. *J. Chem. Soc., Dalton Trans.* **1999**, 2133−2139. Huddleston, J. G.; Broker, G. A.; Willauer, H. D.; Rogers, R. D. ACS Symposium Series 818; American Chemical Society: Washington, DC, 2002; pp 270−288. Seddon, K. R.; Stark, A.; Torres, M. J. ACS Symposium Series 819; American Chemical Society: Washington, DC, 2002; pp 34−49. Dzyuba, S. V.; Bartsch, R. A. *Tetrahedron Lett.* **2002**, *43*, 4657−4659. Headley, A. D.; Jackson, N. M. *J. Phys. Org. Chem.* **2002**, *15*, 52−55.
(31) Yadav, J. S.; Reddy, B. V. S.; Raju, A. K. *Synthesis* **2003**, *6*, 883−886. Laali, K. K.; Borodkin, G. I. *J. Chem. Soc., Perkin Trans.* **2002**, *2*, 953−957. Scott, M. P.; Brazel, C. S.; Benton, M. G.; Mays, J. W.; Holbrey, J. D.; Rogers, R. D. *Chem. Commun.* **2002**, *13*, 1370−1371. Swatloski, R. P.; Spear, S. K.; Holbrey, J. D.; Rogers, R. D. *J. Am. Chem. Soc.* **2002**, *124*, 4974−4975. Togo, H.; Hirai, T. *Synlett* **2003**, *5*, 702−704. Carmichael, A. J.; Adrian, J.; Haddleton, D. M.; Bon, S. A. F.; Seddon, K. R. *Chem. Commun.* **2000**, *14*, 1237−1238.
(32) Law, G.; Watson, P. R. *Langmuir* **2001**, *17*, 6138−6141.
(33) Law, G.; Watson, P. R. *Chem. Phys. Lett.* **2001**, *345*, 1−4.
(34) Law, G.; Watson, P. R.; Carmichael, A. J.; Seddon, K. R. *Chem. Phys. Phys. Chem.* **2001**, *3*, 2879−2885.
(35) Gannon, T. J.; Law, G.; Watson, P. R. *Langmuir* **1999**, *15*, 8429−8434.
(36) Iimori, T.; Iwahashi, T.; Ishii, H.; Seki, K.; Ouchi, Y.; Ozawa, R.; Hamaguchi, H.; Kim, D. *Chem. Phys. Lett.* **2004**, *389*, 321−326.
(37) Carmichael, A. J.; Hardacre, C.; Holbrey, J. D.; Nieuwenhuyzen, M.; Seddon, K. R. *Mol. Phys.* **2001**, *99*, 795−800.
(38) Baldelli, S. *J. Phys. Chem. B* **2003**, *107*, 6148−6152.

surfaces, using synchrotron-based surface-specific X-ray techniques, which are among the most powerful methods for investigating liquid surfaces with angstrom-scale resolution.[40−42] To the best of our knowledge, no X-ray reflectivity (XR) study of the surface of a macroscopic IL sample has been reported to date for any IL. A single XR study of *thin-films* of ILs, spin-coated onto a Si substrate, was reported by Carmichael et al.[37] However, the surface structure of a 100−200 Å film may differ significantly from that of the surface of a semi-infinite liquid bulk, addressed here. More importantly, the ILs studied by Carmichael et al. have much longer alkyl tails (12 and 18 carbons) than the 4-carbon ones studied here. The much larger geometrical anisotropy of the molecules used by Carmichael et al. is therefore more likely to cause liquid-crystalline phases, especially when confined to a thin film configuration, the thickness of which is a few molecular lengths only.

Our measurements indicate the existence of surface layering in the ILs. ST measurements, crucial for the interpretation of the experimental data, are presented as well.

II. Experimental Section

The experimental details have been deposited as Supporting Information.

III. Results

The surface tension (ST) determines the surface roughening arising from the thermally excited capillary waves. As shown below, the confident extraction of the intrinsic surface-normal density profile of the IL from the X-ray reflectivity data sensitively depends, therefore, on the knowledge of the ST. We have measured the surface tension of our samples as a function of temperature in our range of interest. These measurements are discussed next, followed by a discussion of the X-ray reflectivity (XR) results.

A. Surface Tension. The measured temperature-dependent surface tensions $\gamma(T)$ of [bmim][PF_6] and [bmim][BF_4] are shown in Figure 2 (bold lines). Absolute measurements of ST, while being a classical technique, are by no means straightforward. The extreme sensitivity of absolute ST values to tiny amounts of surface impurities (unobservable by X-ray methods), the wetting properties of the different materials used for the DuNouy ring or for the Wilhelmy plate, the depth of immersion of the plate (requiring a correction for the Archimedes force) are only a few of the problems one needs to overcome or correct for in absolute ST measurements. Taking these factors into account, the experimental uncertainty in the absolute values plotted in Figure 2 is $\pm$ 0.6 mJ/m^2. The resolution, i.e., the uncertainty in the relative values, is smaller by at least an order of magnitude.

We know of only two previous surface tension measurements for [bmim][BF_4] and three previous measurements for [bmim][PF_6]. The first, by Huddleston et al.,[29] provides only room-temperature ST values, shown in Figure 2 in triangles. The ST of [bmim][PF_6] was measured for both a sample left to

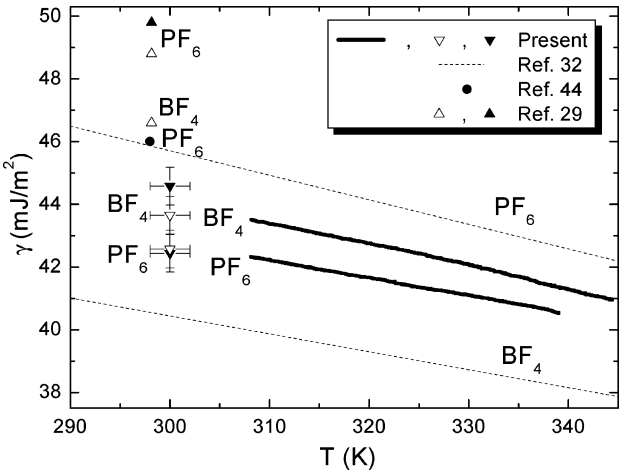

Figure 2. Measured temperature dependence of the surface tension (bold lines) of [bmim][BF_4] and [bmim][PF_6]. The linear fits by Law and Watson[32] to their measured curves are shown in a dashed line. The ambient-temperature ST results of Huddleston et al.[29] are plotted in triangles, the full triangle corresponding to a measurement in a water-equilibrated atmosphere and an open triangle being used for data obtained in a dry atmosphere. Our room-temperature data is shown in inverted triangles, the open triangle is for a sample measured after drying at a vacuum of 40 mTorr at 80 °C for 9 h, and the full triangle is for the same sample, after sitting in a saturated-humidity atmosphere for 12 h. For details see the Supporting Information. The [bmim][PF_6] result of Dzyuba et al.[44] is plotted in full circles.

equilibrate in a water-saturated atmosphere (solid triangle) and in a sample kept in a dry atmosphere (open triangle). The results differ by ~1 mJ/m^2. Both values are ~6 mJ/m^2 higher than our results. The difference may stem from the fact that the absolute values of Huddleston et al. were obtained by scaling their measured values by a constant factor. The factor was selected so as to make the surface tension of a water sample, measured with the same apparatus, to coincide with the literature value.[29] We did not use such a scaling method but set the instrument up so that it measures the absolute value directly.

The linear fits to the ST values quoted by Law and Watson[32] are shown in Figure 2 as dashed lines, so that our [bmim][BF_4] ST falls between the two published results, while our ST of [bmim][PF_6] underestimates the corresponding value of Law and Watson by ~2 mJ/m^2, again, possibly due to their scaling method.[32] The third surface tension study of [bmim][PF_6] is published by Dzyuba and Bartsch,[44] yielding (at room temperature) a value close to that of Law and Watson. Note that, while the first two groups used a DuNuoy ring for the ST studies, Dzyuba and Bartsch measured the ST by a capillary rise method. By assigning the difference in the measured surface tensions, $\Delta\gamma$ to an increase in the surface concentration of impurities, Γ, an estimate can be obtained for Γ from the well-known equation-of-state of the 2D ideal gas,[9] $\Gamma = \Delta\gamma/(k_B)$. The small $\Delta\gamma \approx$ 6 mN/m^2 difference between the Huddleston et al.[29] and our results, if assigned entirely to impurities at the surface, would require an impurity concentration of $\Gamma \approx 10^{-2}$ molecules/Å^2, indicating that the surface tension is indeed sensitive to the adsorbed impurities, as mentioned above. However, this Γ value is only an upper limit for the real difference in the surface

(39) Kakiuchi, T.; Shigematsu, F.; Kasahara, T.; Nishi, N.; Yamamoto, M. *Phys. Chem. Chem. Phys.* **2004**, *6*, 4445−4449.
(40) Deutsch, M.; Ocko, B. M. In *Encyclopedia of Applied Physics*; Trigg, G. L., Ed.; VCH: New York, 1998; Vol. 23, p 479−490.
(41) Als-Nielsen, J.; McMorrow, D. *Elements of Modern X-ray Physics*; Wiley: New York, 2001.
(42) Tidswell, I. M.; Ocko, B. M.; Pershan, P. S.; Wasserman, S. R.; Whitesides, G. M.; Axe, J. D. *Phys. Rev. B* **1990**, *41*, 1111−1128.
(43) An X-ray reflectivity study of thin films of ILs, spin-coated on a Si substrate, was published.[37] However, the behavior of a 100−200 Å film may (and does) differ significantly from the behavior of the surface of a semi-infinite bulk.
(44) Dzyuba, S. V.; Bartsch, R. A. *ChemPhysChem* **2002**, *3*, 161−166.

impurity concentrations, since there are other factors which reduce the ST, as mentioned above. It should be noted that the capillary wave theory (CWT) prediction for the effective surface roughness, σ_{eff}, discussed below, is not very sensitive to the accurate value of the surface tension, since $\sigma_{\text{eff}} \sim \gamma^{-1/2}$ as shown in eq 4.

In a simple monocomponent liquid a negative slope of $\gamma(T)$ is indicative of a surface entropy higher than that of the bulk, while a change to a positive slope would indicate a reduction in the surface entropy below that of the liquid bulk.[12,13] However, this simple signature of surface ordering may have to be modified for a multicomponent liquid, since the relative concentration of the constituents may be different at the surface and in the bulk. Moreover, the concentrations may also be temperature dependent. Indeed, the ST of liquid metals, despite having a measure of order at its surface (i.e., layering), still exhibits $d\gamma/dT < 0$. The slopes of the ILs shown in Figure 2 are close to, albeit slightly lower than, those obtained for surfaces of disordered vdW liquids.[12,45]

B. X-ray Reflectivity. The X-ray reflectivity, $R(q_z)$, is the incident-intensity-normalized surface-reflected intensity measured as a function of the surface-normal component of the wave vector transfer, $q_z = (4\pi/\lambda)\sin(\alpha)$, where α is the grazing angle of incidence of the X-ray beam onto the surface. The measured $R(q_z)$ is shown in Figure 3 for [bmim][BF_4] and [bmim][PF_6]. It exhibits a fast, q_z^{-4}, decay with q_z. For our q_z range, the reflectivity decays by almost 10 orders of magnitude. A very high incident X-ray flux is therefore required to provide acceptable signal-to-background ratios at high incidence angles, α. The well-known Fresnel reflectivity for an ideally flat and abrupt surface is:

$$R_F(q_z) = \left|\frac{q_z - (q_z^2 - q_c^2)^{1/2}}{q_z + (q_z^2 - q_c^2)^{1/2}}\right|^2 \quad (1)$$

where q_c is the critical q_z for total external reflection of X-rays from the surface. For the wavelengths used, $q_c \approx 0.023$ and 0.024 Å^{-1} for [bmim][BF_4] and [bmim][PF_6], respectively. The $R_F(q_z)$ curves, shown for both ILs in Figure 3 in dashed−dotted lines, correspond well to the experimental data at low q_z but deviate significantly from it at $q_z \gtrsim 5q_c$. At high q_z values the microscopic roughness of the liquid surface, due to thermally excited capillary waves, significantly reduces the measured reflectivity relative to R_F. This is a well-known effect, common to all X-ray reflectivity studies of liquid surfaces.

The surface roughness is accounted for by the capillary wave theory.[21,40,41,46] The core of this theory is the balance between the surface tension and the gravitation that limit the interfacial distortions on one hand, and the entropy gain due to these distortions on the other hand. The CWT is a continuum theory, assuming the macroscopic ST to be applicable down to the molecular dimensions. Surprisingly, with only rare and few exceptions,[47] liquid surfaces in general are described very well

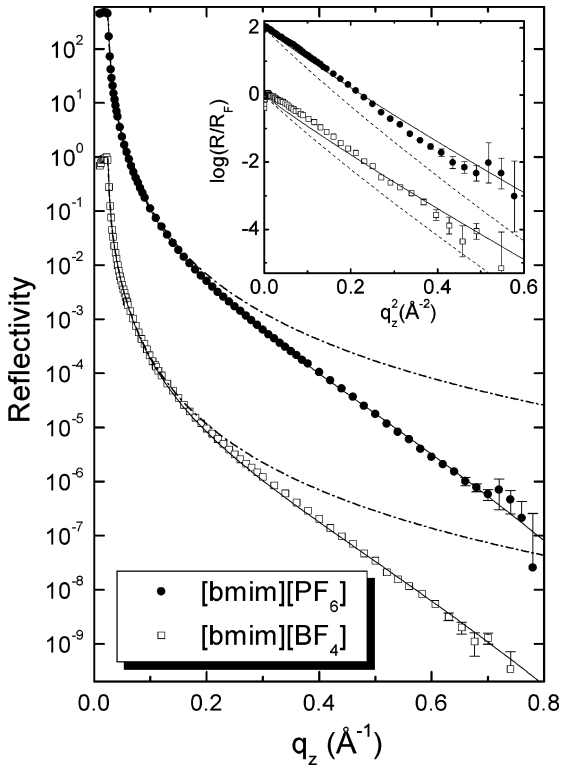

Figure 3. X-ray reflectivity off the [bmim][PF_6] (solid circles) and the [bmim][BF_4] (open squares) surfaces. The [bmim][PF_6] curves are upshifted for clarity by a factor of 500. The theoretical ideal-surface Fresnel reflectivity is shown by dash−dotted lines. The capillary wave theory (CWT) reflectivity fits, described in the text, are shown in solid lines. The γ_{eff} values required to fit the data with this approach are much higher than the directly measured ones. (Inset) The same data normalized to the Fresnel reflectivity off an ideal surface, R_F, vs q_z^2. The [bmim][PF_6] data are shifted up for clarity. The dashed lines indicate the CWT prediction for the measured surface tension of the ILs. The CWT fits, allowing the effective surface tension to vary rather than using the measured surface tension, are shown in solid lines. Note the slight oscillation of the experimental data about the almost linear fits.

quantitatively by the CWT down to molecular length scales.[22] The capillary waves at the surface give rise to nonspecular diffuse scattering, so that the intensity measured at any point in q-space requires an integration in the surface-normal (q_z) and surface-parallel (q_{xy}) directions over the q-resolution of the detector, q_{res}. Thus, the reflectivity measured with the detector being at the specular position at a nominal $q_z \neq 0$, $q_{xy} = 0$ is given by:[21,41,48,49]

$$R(q_z) = \frac{1}{\sin\alpha}\left(\frac{q_c}{2}\right)^4 \frac{\eta}{8\pi q_z^2}|\Phi(q_z)|^2 \int_{\text{res}} \frac{1}{q_{xy}^2}\left(\frac{q_{xy}}{q_{\max}}\right)^{\eta} d^2q_{xy} \quad (2)$$

where $\Phi(q_z)$ is the structure factor of the surface, equal to unity for a simple liquid surfaces lacking intrinsic structure beyond a monotonic increase in the electron density across the surface, $q_{\max} \approx \pi/a$ is the upper wave vector cutoff, due to the finite diameter, a, of the molecules, and $\eta = k_B T q_z^2/(2\pi\gamma)$, where γ is the ST. In addition to the thermally excited capillary waves, there is a small intrinsic surface roughness ($\sigma_0 \approx 1$ Å), which can be taken into account by multiplying eq 2 by $\exp(-q_z^2\sigma_0^2)$.

(45) Ocko, B. M.; Wu, X. Z.; Sirota, E. B.; Sinha, S. K.; Deutsch, M. *Phys. Rev. Lett.* **1994**, *72*, 242−245.
(46) Braslau, A.; Pershan, P. S.; Swislow, G.; Ocko, B. M.; Als-Nielsen, J. *Phys. Rev. A* **1988**, *38*, 2457−2470. Sanyal, M. K.; Sinha, S. K.; Huang, K. G.; Ocko, B. M. *Phys. Rev. Lett.* **1991**, *66*, 628−631.
(47) Luo, G.; Malkova, S.; Pingali, S. V.; Schultz, D. G.; Lin, B.; Meron, M.; Graber, T. J.; Gebhardt, J.; Vanysek, P.; Schlossman, M. L. *Faraday Discuss.* **2005**, *129*, 23−34.
(48) Pershan, P. S.; Braslau, A.; Weiss, A. H.; Als-Nielsen, J. *Phys. Rev. A* **1987**, *35*, 4800−4813.
(49) Shpyrko, O. Ph.D. Thesis, Harvard University, 2004 (unpublished).

The expression obtained for the reflectivity from eq 2, with σ_0 included, can be well approximated as:[21,41,48,49]

$$R(q_z) = R_F(q_z)|\Phi(q_z)|^2 \exp(-q_z^2\,\sigma_{eff}^2) \quad (3)$$

where the effective roughness $\sigma_{eff} = (\sigma_0^2 + \sigma_{CWT}^2)^{1/2}$ with

$$\sigma_{CWT}^2 = \frac{k_B T}{2\pi\gamma}\ln\left(\frac{q_{max}}{q_{res}}\right) \quad (4)$$

Equation 3 indicates that for a simple, unstructured liquid surface (where $|\Phi(q_z)| = 1$) broadened by capillary waves a plot of the data as $\ln[R/R_F]$ vs q_z^2 should yield a straight line with a slope of $-\sigma_{eff}^2$. The inset to Figure 3 shows the data measured for [bmim][PF_6] and [bmim][BF_4] plotted this way. The slopes are equal to -9.0 Å^2 for both ILs. These experimentally derived slopes can be compared with the σ_{eff} value calculated from eq 4 using the independently measured surface tension discussed above.[50] This provides an important test for the validity of the model adopted below for the structure of the surface.

Thus, assuming a simple, unstructured ($|\Phi(q_z)|^2 = 1$), monotonic density profile for our samples, broadened only by capillary waves, as found, for example for water,[22] organic solvents,[46] and alkane melts above their surface-freezing temperatures,[12] and using the measured $\gamma(T)$ of Figure 2, we obtain from eq 2 the dashed line shown in the inset to Figure 3. This line clearly and significantly underestimates the measured reflectivity. Using γ as a free parameter in eq 2 to fit the measured $R(q_z)$ yields $R_{fit}(q_z)$, shown in solid lines in the inset and main Figure 3. While this curve shows a better agreement with the measurements, the agreement is achieved at the cost of an unrealistically high best-fit value of $\gamma = 59.7$ mJ/m^2 for [bmim][PF_6] and $\gamma = 56.3$ mJ/m^2 for [bmim][BF_4]. These values exceed the measured ones by much more than the experimental uncertainty of the surface tension measurements discussed above. A similar underestimation of the surface roughness by the CWT was recently observed for glycerol,[51] leading one to suspect that some of the modes of the capillary waves may be diminished due to the high viscosity of the liquid. While such effect is in principle possible here, recent studies of glass-forming polymeric fluids[52] show that even for these highly viscous fluids the roughness is well described by the usual capillary wave theory. The unphysical γ values obtained above from the fits to CWT argue strongly against a simple monotonic model for the surface density profile. Moreover, a careful examination of the inset to Figure 3 reveals that even employing these high γ values, the measured reflectivity still oscillates around the best-fit line. These oscillations are observed more clearly in a plot of the ratio of the measured reflectivity, $R(q_z)$ to the fitted curve $R_{fit}(q_z)$. This plot is shown in Figure 4 in open circles, and the large deviation from the simple monotonic interface model, ~20% for [bmim][PF_6] and ~30% for [bmim][BF_4], are clearly observed. Such deviations argue strongly in favor of a nonmonotonic density profile with $|\Phi(q_z)|^2 \neq 1$.

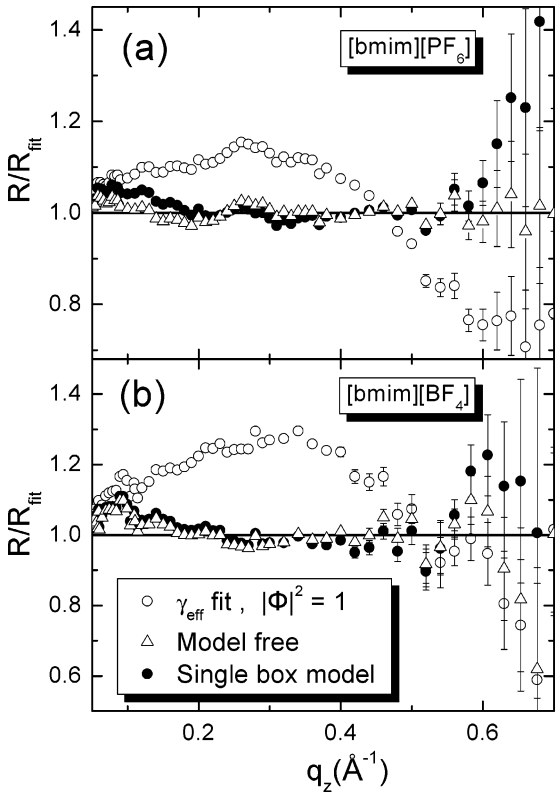

Figure 4. Measured reflectivity $R(q_z)$ for (a) [bmim][PF_6] and (b) [bmim][BF_4], divided by the fitted reflectivity, $R_{fit}(q_z)$ for a monotonic surface density profile with $|\Phi(q_z)|^2 = 1$, broadened by capillary waves (open circles). Note the significant deviations from unity (solid line), indicating that $|\Phi(q_z)|^2 \neq 1$. The deviations are much reduced for the model-free (triangles) and the single-box model (solid circles) fits, both of which indicate a layering at the interface. For a discussion see text.

The structure factor $\Phi(q_z)$ is given by:

$$\Phi(q_z) = \int_0^\infty \frac{d\langle\rho\rangle_{xy}}{dz}\exp(iqz)dz \quad (5)$$

where $\rho(z)$ is the surface-normal density profile averaged in the surface-parallel directions ($\langle\ldots\rangle_{xy}$). As $R(q_z)$ in eq 2 depends on $|\Phi|^2$, the phase information of Φ is lost, as in all conventional X-ray diffraction experiments. This well-known "phase problem"[41] does not allow a unique determination of $\rho(z)$ from $R(q_z)$ alone. The common practice, therefore, is to construct a model for $\rho(z)$, using practical physical and chemical considerations, calculate the structure factor of this model using eq 5, and adjust the parameters of the model by a computer fit to obtain agreement with the measured $R(q_z)$.[12,13,42] Choosing a physically motivated model for $\rho(z)$ may be an easy task when the general structure of the surface is known or when reliable theoretical predictions are available. In our case, however, it is unclear, a priori, whether $\rho(z)$ should exhibit oscillations, decaying into the bulk (as for liquid metals[19,20,21]), a single high-density layer at the surface (as for surface freezing in alkanes[12]), or a more complex, completely different structure.[13] Thus, we have employed first a different technique, the so-called Model-Free algorithm, proposed by Chou et al.[53] This algorithm consists of approximating the (unknown) density profile by a number of "boxes" of fixed widths, fitting the corresponding calculated

(50) Since σ_{CWT} depends only logarithmically on q_{max}, an approximate value of q_{max} is sufficient to calculate reliably the roughness.
(51) Seydel, T.; Tolan, M.; Ocko, B. M.; Seeck, O. H.; Weber, R.; DiMasi, E.; Press: W. *Phys. Rev. E* **2002**, *65*, 184207.
(52) Sprung, M.; Seydel, T.; Gutt, C.; Weber, R.; DiMasi, E.; Madsen, A.; Tolan, M. *Phys. Rev. E* **2004**, *70*, 051809.
(53) Chou, C. H.; Regan, M. J.; Pershan, P. S.; Zhou, X. L. *Phys. Rev. E* **1997**, *55*, 7212−7216.

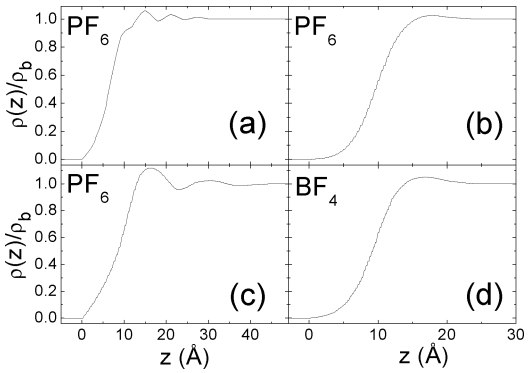

Figure 5. Surface-normal electron density profiles obtained from the fits to the measured $R(q_z)$ using the model-free algorithm for [bmim][PF_6] (a−c) and for [bmim][BF_4] (d). Note the small $d\langle\rho(z)\rangle_{xy}/dz$ discontinuities at $z = 0$ in (a) and (c), as well as the too-fine structure of the profile in (a) which exceed the experimental resolution. These are discussed in the text.

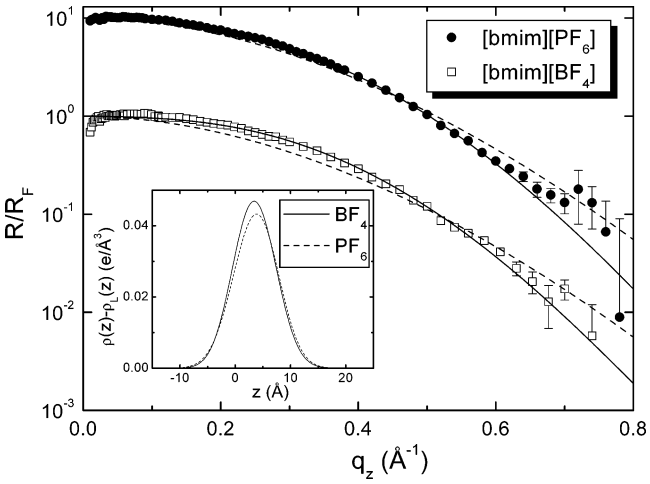

Figure 6. Measured Fresnel-normalized reflectivities. The [bmim][PF_6] data are shifted up, for clarity, by a factor of 10. The $|\Phi(q_z)| = 1$ fits, which yield a reasonable agreement with the measurements but unrealistically high surface tensions are shown in dashed lines. The single-box model fits discussed in the text are shown in solid lines, exhibiting a better fit. The deviations between the single-box model profiles and the monotonic unstructured simple surface profiles are shown in the inset. The single-box model parameters are given in Table 1.

Table 1. Surface Layer's Thickness D and the Surface Electron Density ρ_s, Obtained from the Fits of the Measured $R(q_z)$ by a Single-Box Model for [bmim][PF_6] and [bmim][BF_4]

sample	D Å[a]	ρ_s e/Å^3 [a]	ρ_b e/Å^3 [b]
[bmim][PF_6]	5.8 ± 0.5	0.50 ± 0.01	0.42
[bmim][BF_4]	6.5 ± 0.5	0.45 ± 0.01	0.38

[a] The errors quoted are derived from the parameter values obtained from fits to two sets of XR measurements for each IL, one carried out at NSLS and the other at APS. For details of the measurements see Supporting Information. [b] The bulk electron densities, ρ_b, are calculated from the mass densities reported by the samples' samples.

reflectivity to the measured one, and then automatically increasing the number of boxes, to obtain a smoother profile. The cycle is repeated, until a convergence to a stationary profile is obtained. The great advantage of this algorithm is that, in general, very good fits are obtained to even the most complicated reflectivity curves. In addition to the absence of the phase information, which is manifested in the non-uniqueness of the density profiles obtained, local fitting minima may result in convergence to different profiles for different initial parameters and/or different constraints on the algorithm. An extensive search for different possible $\rho(z)$ solutions that would fit well the measured $R(q_z)$ resulted in the three curves shown in Figure 5a−c for [bmim][PF_6] data. While the fit quality for all three is excellent, the profile in Figure 5b should be considered superior to the other two, for two reasons. One reason is ibn Paquda's razor,[54] which prefers the least-complex solution for a problem over the more complex ones. The other reason is that the discontinuities in $d\langle\rho(z)\rangle_{xy}/dz$ at $z = 0$ in the models in Figure 5a,c, and the fine structure in the model of Figure 5a, which is much sharper than the experimental resolution, are all physically unrealistic.

Interestingly, in contrast with the [bmim][PF_6] model-free profiles, the model-free fits for [bmim][BF_4] converge in all cases to the single ρ shown in Figure 5d, which is very similar to the density profile of Figure 5b for [bmim][PF_6]. While this is by no means a proof of uniqueness, it does strengthen the choice of the [bmim][PF_6] profile shown in panel (b) over those in panels (a) and (c). We reiterate that the fits obtained by all model-free fits are excellent, as demonstrated by fact that the ratio $R(q_z)/R_{fit}(q_z)$, plotted in triangles in Figure 4a,b, is close to unity for all q_z, and the deviations from unity are much smaller than those obtained for the monotonic profile fits of Figure 3, plotted in Figure 4 in open circles.

While the model-free algorithm results in good fits, it does not allow a separation of the surface roughening (due mostly to the thermally excited capillary waves) from the intrinsic, unroughened surface profile. Such a separation is desirable for identifying the ordering of the molecules at, and the physics which determines the structure of, the surface. A separation of these two effects can be done by employing a box model to describe $\rho(z)$. Since the deviation of the chosen profiles in Figure 5b and d from a constant density are small, a single-box model,[42] where a single layer of density ρ_s, higher than that of the bulk ρ_b, resides on top of a simple unstructured surface, was used. In this case:

$$|\Phi(q_z)|^2 = [\tilde{\rho}^2 + (1-\tilde{\rho})^2 + 2\,\tilde{\rho}(1-\tilde{\rho})\cos(q_z D)]\exp(-q_z^2\,\sigma_0^2) \quad (6)$$

where $\tilde{\rho} \equiv \rho_s/\rho_b$ is the surface layer electron density normalized to the bulk liquid electron density and D is the surface layer's thickness. The intrinsic roughness σ_0, which describe noncapillary contributions to the surface roughness, is arbitrarily set to 1 Å, a value used for molecules of this size in several earlier studies.[12,13,21,22,49] Note, however, that as shown above in eq 3, to a very good approximation, the reflectivity is dependent only on $\sigma_{eff} = \sqrt{\sigma_{CWT}^2 + \sigma_0^2}$. For our system, $\sigma_{CWT} \approx 3\sigma_0$, so that the results are very insensitive to the exact value adopted for σ_0, since $\sigma_{eff} \approx \sigma_{CWT}$. As σ_{CWT} is calculated from the known surface tension γ, the only fit parameters in this model are the surface layer's normalized density, $\tilde{\rho}$, and thickness D. The fits of this model to the measured $R(q_z)$ are shown in Figure 6 (solid lines) and the corresponding parameters are given in Table 1. The fits using the (unphysically large) γ_{eff} and a simple unstructured monotonic surface profile ($|\Phi(q_z)| = 1$), discussed above, are

(54) Bahye ibn Paquda, *Kitab al-Hidaya ila Farai'd al-Hulub*; Vol. 1, Chapter 7. This book was published around 1040, three centuries before William of Ockham's 14th century rule of parsimony, "plurality should not be assumed without necessity", which came to be known as "Occam's razor".

also shown in dashed lines for comparison. As can be observed, the single-box model fits the measured $R(q_z)$ much better. The fit ratios $R(q_z)/R_{fit}(q_z)$ of this model, shown in Figure 4 in solid circles, are very close to unity and almost coincide with those of the model-free fits. The resultant density profiles are indistinguishable from those of Figure 5b,d on the scale of the figure. A plot of $(\rho(z) - \rho_L(z))$ is shown in the inset to Figure 6. Here $\rho_L(z)$ is a step-function density profile, for which $|\Phi(q_z)| = 1$, broadened by a roughness of $\sqrt{\sigma_{CWT}^2+\sigma_0^2}$, where $\sigma_0 = 1$ Å, and σ_{CWT} is calculated from the measured surface tension. The ~10%-enhanced density at the surface, *as compared to an unstructured surface*, is clearly observed and is further discussed below.

IV. Discussion

While the surface structure observed is qualitatively similar for both ILs, the [bmim][BF_4] exhibits a larger density enhancement at the surface (inset of Figure 6). Note, however, that the ratio of the surface electron density *to that of the bulk* is equal for both materials, $\tilde{\rho} = 1.18$ (see Table 1). The density of the surface layers, ≥ 0.45 e/Å^3, as listed in Table 1, is much higher than that of densely packed alkanes (0.32 e/Å^3 for solid alkanes[55]) or of water[22] (0.33 e/Å^3), indicating that the enhancement is not likely to be due to these common contaminants. Several tests for a few other possible contaminants, with negative results, were also carried out and are detailed in the Supporting Information. The electron density[56] of liquid 1-methylimidazole is ~0.33 e/Å^3, so that a layer comprising $[bmim]^+$ cations only would have a density of $\rho_{bmim} \approx 0.31$ e/Å^3. The much higher electron density obtained from the XR fits indicates that the surface layer cannot consist solely of cations. Moreover, the difference in the electron density between the surface layers of [bmim][BF_4] and [bmim][PF_6], which have the same $[bmim]^+$ cation, should stem from the different size, and number of electrons, of the respective anions. Using the ionic radii of PF_6^- (2.76 Å)[57] and BF_4^- (2.20 Å),[58] we obtain the electron densities of $\rho_{PF_6} \approx 0.78$ e/Å^3 and $\rho_{BF_4} \approx 0.92$ e/Å^3 for the two anions, respectively.[59]

While the *number* fraction of the anions and the cations in the bulk is equal to 0.5 in our ILs, because of the electroneutrality, the bulk *volume* fractions can be calculated as $x_{PF_6} \approx 0.25$ and $x_{BF_4} \approx 0.14$ for the [bmim][PF_6] and [bmim][BF_4], respectively. Adopting the reasonable assumption that the ratio, A, between the bulk and the surface densities of the anion is the same for the two ILs, we obtain two simple equations:

$$\rho_{[bmim][PF_6]} = (1 - Ax_{PF_6})\rho_{bmim} + Ax_{PF_6}\rho_{PF_6}$$
$$\rho_{[bmim][BF_4]} = (1 - Ax_{BF_4})\rho_{bmim} + Ax_{BF_4}\rho_{BF_4} \qquad (7)$$

where $\rho_{[bmim][PF_6]}$ and $\rho_{[bmim][BF_4]}$ are the surface electron densities of [bmim][PF_6] and [bmim][BF_4], respectively, given in Table 1. Solving these equations for A and ρ_{bmim} yields $A = 1.6 \pm 0.2$, which indicates that the free surface of an IL should have a net negative charge.[60] We are not aware of any surface potential measurements for ILs. These should allow a direct observation of the charge at the surface.

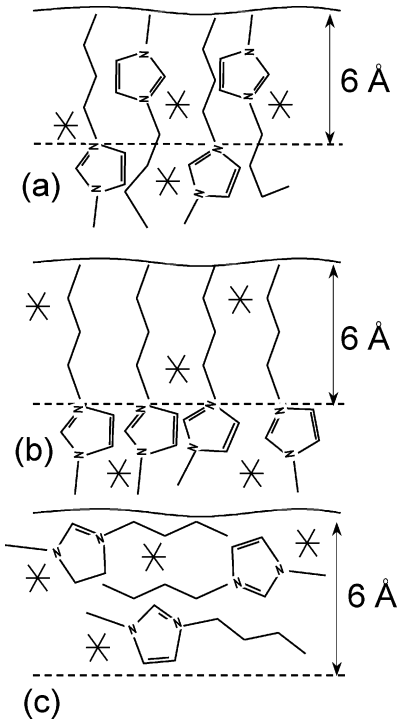

Figure 7. Different possible molecular arrangements of [bmim][PF_6] within the surface-enhanced layer, consistent with the XR results. The six-arm stars symbolize the PF_6^- anions, and the wavy line is the surface. Note that for (b) a significant incorporation of the anions into the hydrophobic layer of butyl tails would be needed to account for the high electron density obtained from the XR fits. As discussed in the text, such an arrangement is not very likely.

Equations 7 also yield $\rho_{bmim} = 0.31 \pm 0.03$ e/Å^3. This value closely corresponds to the upper limit estimate of the electron density of the $[bmim]^+$ cation, 0.315 e/Å^3, obtained by taking the average between the electron densities of the *solid* butane tails[55] (0.30 e/Å^3) and the 1-methylimidazole heads[56] (0.33 e/Å^3).

The thickness of the surface layer (6−7 Å, see Table 1) is close to the length of the butyl tail, implying that the surface layer may comprise standing up molecules, as shown in the two upper panels (a,b) of Figure 7. Note however, that a stack of two to three layers of lying-down molecules, as shown in the lower panel, Figure 7c, cannot be excluded by the present XR measurements, since the thickness of single lying-down layers of this type is below the experimental resolution limit. In addition, sum-frequency vibrational spectroscopy[62] reveals a significant incorporation of *p*-tosylate ions into monolayers of $[C_{16}TA]^+$ (cetyltrimethylamonium) on water, despite the hydrophobicity. However, that and the present systems may differ in other, more dominant, interactions. In the arrangement shown in Figure 7b the imidazole groups are excluded from the surface layer. The value obtained for the ρ_{bmim} above requires dense packing of the alkyl tails if no imidazole groups are present in the surface layer. The incorporation of the spherical, charged anions (required to obtain the high $\rho(z) \geq 0.45$ e/Å^3) into such a hydrophobic layer is unlikely, so that the arrangement

(55) Small, D. M. *The Physical Chemistry of Lipids*; Plenum: New York, 1986.
(56) http://www.chemicalland21.com/arokorhi/industrialchem/organic/1-METHYLIMIDAZOLE.htm.
(57) Kato, M.; Takahashi, J.; Sugimoto, Y.; Kosuge, C.; Kishi, S.; Yano, S. *J. Chem. Soc., Dalton Trans.* **2001**, 747−752.
(58) Hofstetter, C.; Pochapsky, T. C. *Magn. Reson. Chem.* **2000**, *38*, 90−94.
(59) These high values are nonphysical, since a purely anionic material would be highly unstable due to the strong Coulombic repulsions between the negatively charged anions.
(60) Jarvis, N. L.; Scheiman, M. A. *J. Phys. Chem.* **1968**, *72*, 74−78.
(61) Kölle, P.; Dronskowski, R. *Eur. J. Inorg. Chem.* **2004**, 2313−2320.
(62) Bell, G. R.; Li, Z. X.; Bain, C. D.; Fischer, P.; Duffy, D. C. *J. Phys. Chem.* B **1998**, *102*, 9461−9472.

in Figure 7b can probably be dismissed. This conclusion is consistent with recent studies of the bulk structure of [bmim][BF_4], which indicate that segregated polar and nonpolar domains are formed even in the liquid state.[61] The XR measurements on thin films of ionic liquids, mentioned in the Introduction, were also interpreted in terms of segregated polar and nonpolar layers,[37] although the strongly anisotropic cations used in that work promote segregation much more intensively than the less elongated cations of the ILs used in the present study.

Finally, it is instructive to compare the electron densities obtained here (see Table 1) with the published solid bulk electron density of 1,3-Dimethylimidazolium hexafluorophosphate ([dmim][PF_6], $C_5H_9N_2-PF_6$). The [dmim][PF_6] has the same molecular structure as [bmim][PF_6], except for a methyl group replacing the butyl tail of [bmim][PF_6]. The electron density of the [dmim][PF_6] crystal (at room temperature) can be calculated from its published[63] crystallographic cell volume as 0.515 e/Å^3, which is only slightly higher than the value obtained here for [bmim][PF_6].

An attempt to add a low-density layer on top of a higher density one, to represent a situation where the hydrophobic tails and polar heads and anions of the molecules segregate into separate layers, failed to yield an acceptable fit to the measured $R(q_z)$. The density of the alkyl layer invariably converged to zero, excluding this type of segregation at the surface. The neutron reflectivity measurements of Bowers et al.,[27] albeit of an inherently lower resolution than the present results due to the smaller q-range, were interpreted *qualitatively* as showing such a segregated profile. Since a *quantitative* analysis of the fitted scattering length density profile in terms of the contributions of the separate molecular moieties was not provided, and because in a multicomponent system like ours the "translation" between the scattering length density profile and an electron density profile is not unique, the two set of results cannot be compared at this stage.

The computer simulations of Lynden-Bell[26] for the IL dimethylimidazolium chloride yield a layered surface with an oscillatory density profile, akin to that observed for liquid metals. Since the functional form of the single-box model cannot yield an oscillatory $\rho(z)$, we have attempted also to fit the measured $R(q_z)$ by a distorted-crystal model.[19,20] This model was developed to describe the density profile of liquid metals and is tailored to describe a sine-wave-like oscillatory density profile, the amplitude of which decays with increasing depth z below the surface. A fit of our measured $R(q_z)$ by this model invariably yields a very short decay length, such that only the first oscillation is observed, and the second one is already too small to observe above the constant bulk density. Consequently, the density profile obtained using this model comes out to be identical, within the scale of the figure, with that obtained from the single-box model shown in Figure 5b and d. We conclude, therefore, that in contrast with liquid metals, the ILs studied here do not exhibit an oscillatory surface electron density profile but only a slight enhancement of the electron density in a 6−7 Å thick surface layer. Note, however, that the dimethylimidazolium chloride IL simulated by Lynden-Bell has more spherical cations than the butyl-tailed cations of both our ILs. The different behavior may therefore reflect the different molecular shape. Clearly, X-ray measurements of the surface structure of dimethylimidazolium chloride, and/or realistic simulations of the surface structure of [bmim][PF_6] and [bmim][BF_4] would be very desirable.

The discussion above leads to the conclusion that the surface-induced density enhancement in the ILs is different from all surface-ordering phenomena observed to date. In contrast with liquid metals, the electron density profile is not oscillatory. In contrast with liquid crystals, and alkanes and their derivatives, the alkyl tails of the [bmim] do not seem to segregate into a separate layer but rather mix with the ions and the charged imidazole rings. Naïvely, one would expect the alkyl tails to segregate to the surface, since their purely vdW interaction should yield a lower surface energy than that of the charged imidazole ring and the anion, which have Coulombic interactions. According to classical theories, an ion-depletion layer should exist near the surface of aqueous salt solutions due to such interactions,[64] and one may therefore expect a polar group depletion layer at the surface of ILs. However, a closer inspection reveals that these theories are valid only for the very low concentration limit, while the absence of a solvent renders our ILs an infinite-concentration "solution". We hope that the results presented here will motivate ab initio theoretical studies in this limit too, which may account for our observations.

V. Conclusions

We presented here the first X-ray reflectivity study of the surface structure of bulk ionic liquids. The analysis demonstrates the existence of a surface layer 6−7 Å thick, of an electron density 10−12% higher than that of an equivalent simple, unstructured liquid surface. The chemical substitution of the anion allowed us to estimate that the increase in the electron density is due to a (15 ± 5)% enhancement in the molar fraction of the PF_6^- and the BF_4^- anions in the surface region, as compared to the 0.5 molar fraction of the bulk. Independent tests of this estimate, perhaps by surface potential measurements, will be most welcome. Two likely molecular arrangements were proposed for the surface layer, one with the butyl chains parallel to the surface and the other with the chains normal to the surface. Both of arrangements differ from the surface ordering observed in other systems to date, namely the oscillatory surface-normal density profiles observed in the liquid metals, the condensed alkyl chain layer in surface-frozen alkanes, and the segregation of the polar and apolar molecular moieties in surface-frozen alcohols and in liquid crystals. Future studies using ILs with moieties accessible to resonant X-ray scattering measurements may help to better elucidate the molecular orientations and positions of the cations and anions within the surface layer. Grazing incidence diffraction measurements are also planned to study the surface-parallel structure in the surface layer and its variation with temperature.

Acknowledgment. Support to M.D. by the U.S.-Israel Binational Science Foundation, Jerusalem is gratefully acknowledged. We thank Chemada Fine Chemicals Ltd., Israel for a supplying the ILs used in this study, and Dr. Y. Rachmilevitch of ICL Industrial Products, Ltd., Israel, for expert Br essays.

(63) Holbrey, J. D.; Reichert, W. M.; Nieuwenhuyzen, W. M.; Sheppard, O.; Hardacre, C.; Rogers, R. D. *Chem. Commun.* **2003**, 476−477.

(64) Onsager, L.; Samaras, N. N. T. *J. Chem. Phys.* **1934**, *2*, 528−536. Landau, L. D. *Statistical Physics*; Nauka: Moscow, 1964.

M.D. gratefully acknowledges useful discussions with Profs. J. Penfold and R.M. Lynden-Bell. B.N.L. is supported by U.S. DOE Contract No. DE-AC02-98CH10886. Work at the CMC Beamlines is supported in part by the Office of Basic Energy Sciences of the U.S. Department of Energy and by the National Science Foundation Division of Materials Research. Use of the Advanced Photon Source is supported by the Office of Basic Energy Sciences of the U.S. Department of Energy under Contract No. W-31-109-Eng-38.)

Supporting Information Available: Experimental details. This material is available free of charge via the Internet at http://pubs.acs.org.

JA0509679